COMMUNICATION

Solvent response of polymers for micromachine manipulation†

Ye Tian,[a] Yong-Lai Zhang,*[a] Hong Xia,[a] Li Guo,[a] Jin-Feng Ku,[a] Yan He,[a] Ran Zhang,[a] Bin-Zong Xu,[a] Qi-Dai Chen[a] and Hong-Bo Sun*[ab]

A novel solvent responsive polymer micromachine has been successfully fabricated by two-photon photopolymerization (TPP) of methacrylate-based photoresists. The moving part of the micromachine could be easily driven by interfacial solvent polarity induced swelling and shrinking of the photopolymer networks. Furthermore, the driving performance of the micromachine could be precisely modulated by varying the laser scanning step length during fabrication.

In recent years, smart micromachines have attracted much attention due to their distinct advantages, such as miniaturized scale, high efficiency, high sensitivity, and low consumption. To date, complex micromachines have been successfully fabricated through novel nanotechnologies,[1,2] such as chemical vapor deposition,[3] two-photon stereolithography[4,5] UV nanoimprint lithography[6] and multiple beam multiphoton polymerization,[7] and they are widely applied in many fields, including biomedical nanotechnology,[8–10] microfluidics,[11,12] nanofriction,[13] analytical chemistry and microsensors.[14,15] Nevertheless, there are still many difficulties in manipulation of these tiny devices in a controlled fashion, and therefore, the driving technologies become the key issue for developing novel micromachines. Current driving schemes, such as electrostatic force,[16,17] piezoelectricity,[18] magnetic fields[19,20] and optical trapping,[21,22] usually suffer from large and complex external cooperative systems, which significantly hinder their practicability in microdevices, for instance, lab-on-a-chip (LoC) systems.

As an alternative solution to micromachine manipulation, stimuli responsive materials (SRMs), which have special responses to environmental conditions (*e.g.* temperature, light, pH value, electric field, metal ions, solvent polarity), have become a hot topic for the fabrication of smart devices.[23–27] For instance, protein hydrogels show pH-responsive properties for microactuation.[28] Azobenzene-based polymers have the novelty of photoinduced deformation, which imparts the opportunity for creating photo-controllable devices.[29,30] In particular, substantial efforts have been devoted to the development of novel SRMs, which are compatible with general microfabrication processes, towards smart surfaces or microstructures. In fact, it is not necessary to pursue SRMs that have special responsive molecules or functional groups to environmental conditions. Microactuation induced morphology change often happens at all kinds of interfaces.[31] Therefore, it is very innovational to utilize novel interfacial actuation for precise manipulation of micromachines fabricated by conventional photopolymers.

In this communication, we report a simple fabrication and manipulation of 3D micromachines *via* two-photon photopolymerization (TPP).[32,33] General methacrylate-based polymers were proved solvent responsive when they were polymerized into microstructures by TPP. The as-formed photopolymer networks have a larger interfacial area to surrounding solvents as compared to bulky polymers. Thus these polymer microstructures could contract or expand sensitively due to the solvents polarity induced swelling and shrinking. In this way, a slipping-block microdevice was successfully manipulated by simple alternation of the solvent environments. Furthermore, for precise control of the micromachines, the shrinkage degree of the microstructures was carefully modulated by changing the scanning step length during the laser processing.

In our experiments, the micromachines were fabricated by two-photon induced photopolymerization of a methacrylate-based photoresist which consisted of butyl methacrylate (BMA, 36 wt%) as monomer, propoxylated trimethylolpropane triacrylate (PO$_3$–TMPTA, 56 wt%) as crosslinker, 2,4,6-trimethylbenzoyldiphenyl phosphine oxide (4 wt%) and phenylbis (2,4,6-trimethylbenzoyl) phosphine oxide (4 wt%) as photoinitiators (for details of the laser fabrication process, see ESI†). To better understand the swelling and shrinking behavior of the photopolymer networks, linear polybutyl methacrylate (for preparation details, see ESI†) was dissolved in various solvents. As shown in Fig. 1a, the PBMA monolith cannot be dissolved in n-hexane and ethanol due to their poor solvency. On the contrary, benzene, ethyl acetate, chloroform and acetone show good solvency for PBMA. It is well known that such linear polymers can dissolve in their 'good' solvents, and precipitate in 'poor' solvents according to the compatibility and similitude principle. Whereas, for the crosslinked polymer networks, the dissolving phenomenon cannot be

[a] State Key Laboratory on Integrated Optoelectronics, College of Electronic Science and Engineering, Jilin University, 2699 Qianjin Street, Changchun 130012, China. E-mail: yonglaizhang@jlu.edu.cn, hbsun@jlu.edu.cn; Fax: 86 431 85168281; Tel: 86 431 85168281
[b] College of Physics, Jilin University, 2699 Qianjin Street, Changchun 130012, China
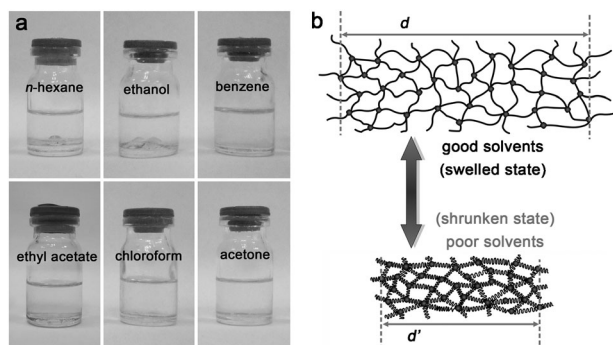
Fig. 1 (a) Photographs of linear polybutyl methacrylate (PBMA) monoliths dissolved in various organic solvents. (b) Scheme of swelling and shrinking of crosslinked polymer networks in good and poor solvents.

observed even if they are treated with 'good' solvents. However, the same principle could still be found, because the polymeric chains between neighbouring crosslinkers behave just like linear polymers at the solvent/polymer interface. In particular, for micrometre-scale polymer wires prepared *via* TPP, the swelling and shrinking phenomenon would be amplified owing to their loose networks and the relatively large interfacial surface area exposed to environmental solvents. As shown in Fig. 1b, the polymer network swells in 'good' solvents, which makes the polymer expand (above). On the contrary, the polymer chains fold and shrink in 'poor' solvents, and thus the polymer contracts (below). As the force that causes the transformation between swelling and shrinking is derived from the interreaction of the solvent and polymer network, approaches to increase of the interfacial area would enhance the sensitivity of this stimulation. Therefore, it is of considerable interest to make full use of this interfacial actuation to drive micromachines in a controlled manner.

In order to test the swelling and shrinking behavior of the photopolymerized microwires, a microstructure that consists of a suspending responsive microwire and two fixed anchors was designed and fabricated *via* TPP. Fig. 2a is the three-dimensional (3D) scheme of this model. In our experiments, we utilized a $60 \times$ oil immersion objective lens with a high numerical aperture (NA = 1.35) to focus the femtosecond laser pulses (wavelength: 790 nm, pulse width: 120 fs, repetition rate: 80 MHz) into the resin. The laser focal spot point was scanned point by point according to the computer program (for details, see ESI†). The laser power of polymerization was 6 mW and scanning step length was 100 nm. After fabrication, the unpolymerized resin was washed out by ethanol. As shown in Fig. 2b, the suspending microwire is straight, and the length between the two anchors in ethanol is measured to be 62.3 μm. Interestingly, when we put it into acetone (Fig. 2c), the microwire expanded noticeably. The length of the microwire became 67.3 μm, about an 8.0% increase in length. In contrast, when the environmental solvent was replaced by n-hexane, the curving microwire between two anchors recovered its straight morphology immediately (Fig. 2d). The length in n-hexane is decreased to 56.1 μm. It is worthy of pointing out that, in this condition, further shrinking of the microwire is limited, because the nanowire

was anchored to the two pillars respectively. As observed from Fig. 2d, there is obvious deformation of the pillars which is caused by the drag of the microwire shrinking. To get further insight into the response properties of this stimulation, the dependence of length change and response time was investigated. As shown in Fig. 2e, in the first period, the response time of elongation (~ 11 μm) was less than 0.1 s, whereas the shrinking time was about 0.5 s. In our test, the responsive microwire was reliable over quite a long time; after repeating for 50 periods, the length changes for both elongation and shrinking almost kept the same value. The response time for elongation was still less than 0.1 s, and the shrinking time was slightly increased to 1.0 s. The different response times for elongation and shrinking are due to the microwire being able to swell freely in acetone, while its shrinking had to overcome the drag force from the fixed pillars.

Taking advantage of this solvent actuation, a slipping-block microdevice was designed and fabricated using the same photoresist and method mentioned above (ESI†). As schematically shown in Fig. 3a, firstly, a cube anchor and a rail were fixed on the substrate. Then, as the moving part, a suspending block which wrapped the rail was linked with the anchor by four microwires. Here, these microwires were assigned as responsive components to pull the moving block along the rail when the solvent environment was changed.

Fig. 3b shows the SEM image of the slipping-block microdevice. The four microwires of the slipping-block device are attached to the substrate due to the removal of solvents. Nevertheless, in the solvent environment, the microwires would suspend, and the block could be pulled away freely (supporting video, ESI†). Fig. 3c shows optical microscopic images of the microdevice in ethanol and n-hexane, respectively. The four microwires were fabricated at 20 nm of laser scanning step length. As shown in the supporting video (ESI†), when the environmental solvents were changed from ethanol to n-hexane, the slipping block was pulled away due to the shrinking of the four microwires. The moving distance of the block was measured to be 3.9 μm. Normally, the moving performance of the slipping block would mainly depend on the diameter of the four microwires, the crosslinking density of the polymer networks and the polarity of environmental solvents. In our experiments, we do not screen for all these influences. It is considered that the laser scanning step length would have an influence on both size and crosslinking density of the polymer microwires. We keep all of the laser processing factors constant and change the step length of laser scanning to obtain different microwires. As shown in Fig. 3d, when a 150 nm step length was adopted for the fabrication, the resulting moving distance of the slipping block was as large as 14.3 μm, about 3.7 times the moving distance of that created with a 20 nm scanning step length. These results indicate the possibility for precisely tuning the driving performance of the microwires.

In order to systematically investigate the shrinking behavior of the microwires, a series of slipping-block microdevices with microwires created at different laser scanning step lengths were successfully fabricated. Then the dependence of step length on the diameter of the microwires, as well as the moving distance of the blocks, were carefully evaluated. As shown in Fig. 4,
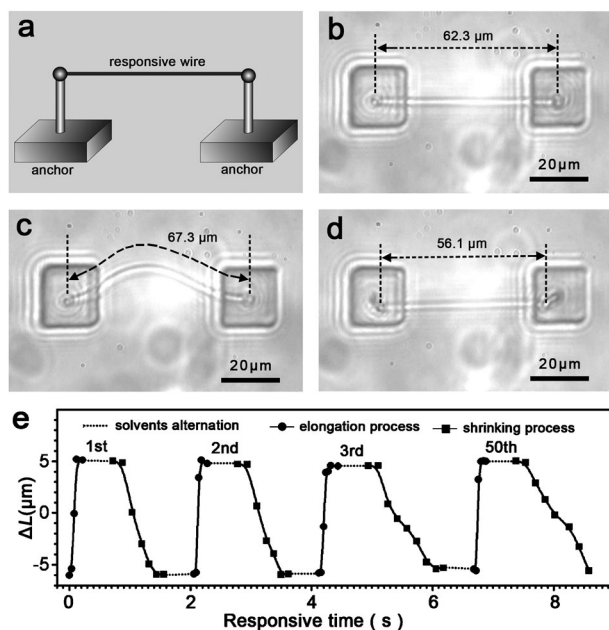
Fig. 2 (a) Sketch of a designed microstructure with two anchors and a connected responsive microwire. (b)–(d) Optical microscopic images of the microstructure in (b) ethanol, (c) acetone and (d) n-hexane. (e) Dependence of length change (ΔL) of the microwire on response time; the dotted lines indicate the time of solvent alternation, which is not the exact time.
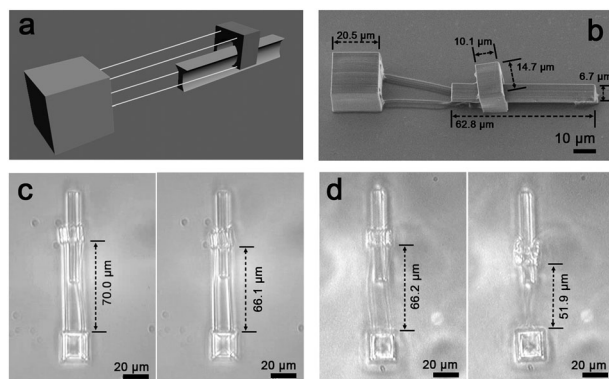

Fig. 3 (a) 3D model of the slipping-block microdevice. (b) SEM image of the slipping-block microdevice. (c) Optical microscopic images of the slipping block with 2.4 µm thick dragging nanowires in ethanol (left) and n-hexane (right). (d) Optical microscopic images of the slipping block with 1.3 µm thick dragging nanowires in ethanol (left) and n-hexane (right).

with the increase of the laser scanning step length from 20 to 200 nm, the diameters of the microwires decrease from 2.4 to 1.2 µm due to the reduction in polymerized region. On the other hand, the moving distance of the block, in other words, the shrinking distance of the microwires increases with the laser scanning step length. Probably, a relatively large shrinking distance would be partly related to the small diameter of the microwires which makes the polymer networks adequately exposed to solvents. More importantly, a larger scanning step length would lead to a low crosslinking density of the polymer networks, which would contribute to a loose
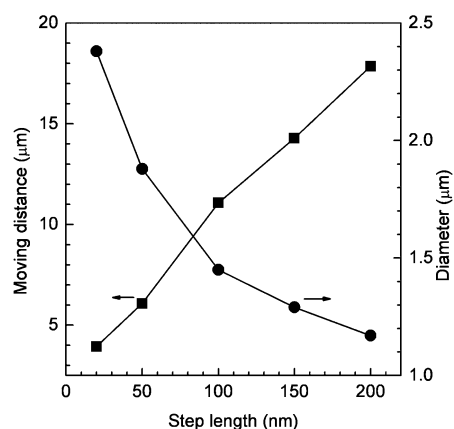

Fig. 4 The dependence of the block's moving distance and the nanowires' diameters on the scanning step length of the laser.

network and therefore significantly increase the interfacial area between polymer networks and surrounding solvents, giving good sensitivity for swelling and shrinking. Both of the effects on diameters and crosslinking density of the microwires are coincident, that is, the larger the step length, the larger the driving distance.

In conclusion, a novel solvent responsive driving mechanism for microactuation of general polymer micromachines was proposed. Methacrylate-based polymer microwires fabricated *via* TPP could swell and shrink in different organic solvents due to the interreaction of interfacial solvents and the photopolymer network. Taking advantage of this solvent effect, a solvent responsive micromachine was fabricated accordingly. The driving behavior of the micromachine could be precisely tuned by controlling the laser scanning step length during fabrication of the sensitive microwires. The solvent responsive micromachines may open up a new driving mechanism for the microactuation of micromachines, and would be potentially important for microdevices such as lab-on-a-chip (LoC) systems and polymer microelectromechanical systems (P-MEMS).

Acknowledgements

References

1 S. Kawata, H. B. Sun, T. Tanaka and K. Takada, *Nature*, 2001, **412**, 697.
2 Y. L. Zhang, Q. D. Chen, H. Xia and H. B. Sun, *Nano Today*, 2010, **5**, 431.
3 M. M. Samani, Y. S. Zhou, W. Xiong, Y. Gao, M. Mitchell, L. Jiang and Y. F. Lu, *Nanotechnology*, 2010, **21**, 395601.
4 S. H. Park, D. Y. Yang and K. S. Lee, *Laser Photonics Rev.*, 2009, **3**, 1–2.
5 S. Juodkazis, V. Mizeikis and H. Misawa, *J. Appl. Phys.*, 2009, **106**, 051101.
6 K. S. Lee, R. H. Kim, D. Y. Yang and S. H. Park, *Prog. Polym. Sci.*, 2008, **33**, 631.
7 X. Z. Dong, Z. S. Zhao and X. M. Duan, *Appl. Phys. Lett.*, 2007, **91**, 124103.
8 E. R. Hitzky, M. Darder, P. Aranda and K. Ariga, *Adv. Mater.*, 2010, **22**, 323.

9 Q. Ji, M. Miyahara, J. P. Hill, S. Acharya, A. Vinu, S. B. Yoon, J. S. Yu, K. Sakamoto and K. Ariga, *J. Am. Chem. Soc.*, 2008, **130**, 2376.

10 Q. Zhua, W. Y. Shih and W. H. Shih, *Sens. Actuators, B*, 2007, **125**, 379.

11 S. Unnikrishnan, H. Jansen, E. Berenschot, B. Mogulkoc and M. Elwenspoek, *Lab Chip*, 2009, **9**, 1966.

12 Y. Tian, Y. L. Zhang, J. F. Ku, Y. He, B. B. Xu, Q. D. Chen, H. Xia and H. B. Sun, *Lab Chip*, 2010, **10**, 2902.

13 D. B. Asay, M. T. Dugger, J. A. Ohlhausen and S. H. Kim, *Langmuir*, 2008, **24**, 155.

14 K. Deisingh, *Analyst*, 2003, **128**, 9.

15 M. Zougagh and Á. Ríos, *Analyst*, 2009, **134**, 1274.

16 G. Keskar, B. Elliott, J. Gaillard, M. J. Skove and A. M. Rao, *Sens. Actuators, A*, 2008, **147**, 203.

17 W. C. Chuang, H. L. Lee, P. Z. Chang and Y. C. Hu, *Sensors*, 2010, **10**, 6149.

18 A. Balasubramanian, M. B. G. Jun, R. E. DeVor and S. G. Kapoor, *J. Manuf. Sci. Eng.*, 2008, **130**, 031113–2.

19 H. Xia, J. Wang, Y. Tian, Q. D. Chen, X. B. Du, Y. L. Zhang, Y. He and H. B. Sun, *Adv. Mater.*, 2010, **22**, 3204.

20 J. Wang, H. Xia, B. B. Xu, L. G. Niu, D. Wu, Q. D. Chen and H. B. Sun, *Opt. Lett.*, 2009, **34**, 581.

21 K. Dholakia and P. Reece, *Nano Today*, 2006, **1**, 18.

22 M. E. J. Friese, H. Rubinsztein-Dunlop, J. Gold, P. Hagberg and D. Hanstorp, *Appl. Phys. Lett.*, 2001, **78**, 547.

23 C. Xia, H. Lee and N. Fang, *J. Micromech. Microeng.*, 2010, **20**, 085030.

24 R. Yerushalmi, A. Scherz, M. E. Boom and H. B. Kraatz, *J. Mater. Chem.*, 2005, **15**, 4480.

25 P. A. L. Fernandes, S. Schmidt, M. Zeiser, A. Feryc and T. Hellweg, *Soft Matter*, 2010, **6**, 3455.

26 T. Tatsuma, K. Takada and T. Miyazaki, *Adv. Mater.*, 2007, **19**, 1249.

27 M. Geoghegan, L. R. Pérez, C. C. Dang, A. J. Parnell, S. J. Martin, J. R. Howse, R. A. L. Jones, R. Golestanian, P. D. Topham, C. J. Crook, A. J. Ryan, D. S. Sivia, J. R. P. Webster and A. Menelle, *Soft Matter*, 2006, **2**, 1076.

28 S. K. Seidlits, C. E. Schmidt and J. B. Sheat, *Adv. Funct. Mater.*, 2009, **19**, 3543.

29 Y. Li, Y. He, X. Tong and X. Wang, *J. Am. Chem. Soc.*, 2005, **127**, 2402.

30 T. Hugel, N. B. Holland, A. Cattani, L. Moroder, M. Seitz and H. E. Gaub, *Science*, 2002, **296**, 1103.

31 M. Sathish, K. Miyazawa, J. P. Hill and K. Ariga, *J. Am. Chem. Soc.*, 2009, **131**, 6372.

32 H. B. Sun and S. Kawata, *Adv. Polymer Sci.*, 2004, **170**, 169.

33 K. D. Belfield, K. J. Schafer, Y. Liu, J. Liu, X. Ren and E. W. V. Stryland, *J. Phys. Org. Chem.*, 2000, **13**, 837.